

Article

## Fibre Coupled Photonic Crystal Cavity Arrays on Transparent Substrates for Spatially Resolved Sensing

Mark G. Scullion \*, Matthias Fischer and Thomas F. Krauss

Department of Physics, University of York, York, YO10 5DD, UK,

E-Mails: matthias.fischer@york.ac.uk (M.F.); thomas.krauss@york.ac.uk (T.F.K.)

\* Author to whom correspondence should be addressed; E-Mail: mark.scullion@york.ac.uk;  
Tel.: +44(0)-1904-322-701.

Received: 14 October 2014; in revised form: 30 October 2014 / Accepted: 30 October 2014 /

Published: 3 November 2014

---

**Abstract:** We introduce a photonic crystal cavity array realised in a silicon thin film and placed on polydimethylsiloxane (PDMS) as a new platform for the *in-situ* sensing of biomedical processes. Using tapered optical fibres, we show that multiple independent cavities within the same waveguide can be excited and their resonance wavelength determined from camera images without the need for a spectrometer. The cavity array platform combines sensing as a function of location with sensing as a function of time.

**Keywords:** photonic crystal sensors; tapered fibre; PDMS transfer

---

### 1. Introduction

Photonic waveguide structures such as ring resonators [1–3], slot waveguides [4] and photonic crystals [5–9] have shown promise as sensors for “lab-on-a-chip” style applications due to their combination of small size and high sensitivity. Typically, these devices are chip-based, which limits their use to laboratory-based applications. In contrast, it is very desirable to develop sensors that can measure living cells and tissue *in-situ*, in order to monitor biomedical processes directly. Such *in-situ* sensors need to be small, flexible and able to directly interface to an optical fibre, such that the fibre becomes the limiting factor of the device size, not the chip. The sensor should be addressable from both sides, *i.e.*, not sit on an opaque substrate. Furthermore, one would like these sensors to be multimodal, *i.e.*, to measure different aspects of the same sample, either by looking for multiple biomarkers or by taking data points at different spatial locations. For example, being able to detect the

secretion or binding of different proteins at different locations on a cell or wound, or the refractive index profile across the breadth of a microfluidic channel.

The photonic crystal cavity array platform we introduce here meets all of these requirements. The platform is based on an array of “hollow” cavities [10,11], each of which is designed for a different resonance wavelength, hence we use the well-known technique of wavelength division multiplexing to address spatially separate cavities; the wavelength separation allows us to either detect different analytes, or to detect different areas of the sample, all through the same fibre channel. Here, as a proof-of-concept demonstration, we demonstrate the operation of an array of photonic crystal cavities mounted on a transparent polydimethylsiloxane (PDMS) substrate. The array is directly connected to a tapered optical fibre via an inverse tapered waveguide. By using a tuneable laser on the input side, we also remove the need for a spectrometer thereby highlighting that the platform, despite its novel functionality, is intrinsically very simple.

## 2. Experimental Section

### 2.1. Photonic Crystal Fabrication and PDMS Transfer

Photonic crystal structures were created in 220 nm top layer silicon-on-insulator (SOI) substrates using the following protocol: ZEP 520-A e-beam resist was spun at 3200 r.p.m. on a small piece of SOI, and baked at 180 °C for 10 min. The desired pattern was then written on the resist in a Raith Voyager 50 kV electron beam writer. After developing for 1 min 25 s in xylene, and rinsing in isopropanol, the pattern was transferred into the silicon via reactive ion etching using a 1:1 blend of CHF<sub>3</sub> and SF<sub>6</sub>. The silicon dioxide below the top silicon layer was then removed using a buffered oxide etch of 1:6 (49%) HF: (40%) NH<sub>4</sub>F for 10 min. To transfer the structure to PDMS, Dow Corning Sylgard 184 was mixed in a ratio of 1.3:10 curing agent:base elastomer by volume, degassed in a desiccator, poured on top of a silanized piece of silicon wafer in a petri dish, and placed in a 60 °C oven for several hours. The cured PDMS was then peeled from the silanized silicon and cut to size with a scalpel. The best results for transferring the photonic crystal waveguide to the PDMS were achieved when an extra step of Piranha cleaning (3:1 H<sub>2</sub>SO<sub>4</sub>:H<sub>2</sub>O<sub>2</sub> for 10 min) of the SOI was first performed. After Piranha clean, the SOI was rinsed in deionized water, followed by acetone and isopropanol. The side of PDMS originally in contact with the silicon PDMS master was then gently dropped on top of the SOI containing the photonic crystal waveguide structures, before firmly pressing down, turning the chip upside down, and placing in a 60 °C oven overnight. The PDMS was then peeled from the SOI, revealing the photonic crystal structures transferred to the PDMS. The photonic crystal remains attached to the rest of the silicon at the top and bottom boundaries of the lattice (see Figure 1) after the oxide etch. The input and output waveguides can bend downwards after oxide etching, but for the 200 micron long waveguides used here they do not break from the rest of the crystal. Yields approaching 100% have been achieved for the transfer of the photonic crystals themselves, whereas for the input and output waveguides, this is closer to 50%. Initial work suggests that placing periodic vertical supports (300–500 nm wide) along the length of the waveguides can result in higher yields and longer waveguides being transferred.

## 2.2. Tapered Fibre Fabrication

Tapered optical fibres were prepared using the following method: An SMF28e single mode fibre with FC/PC connectors was cut in half using a scalpel. A small length of the outer jacket was then removed via a small incision with the scalpel and gently pulled apart. The protective Kevlar threads were then cut. To remove the inner jacket, an incision was made on either side with the scalpel, and the fibre immersed in paint stripper (Nitromors®) to soften it, before gently pulling it off. The acrylic coating was then removed by gently scraping along one side of the fibre, immersing again in Nitromors, and wiping along the fibre with lens tissue. The exposed end of the fibre was then attached to a gantry and a 20 g weight attached to the fibre end. The exposed region of the fibre was then heated with a propane blow torch, the fibre stretching under the influence of the attached weight, thus naturally forming two tapered fibre ends.

## 3. Results and Discussion

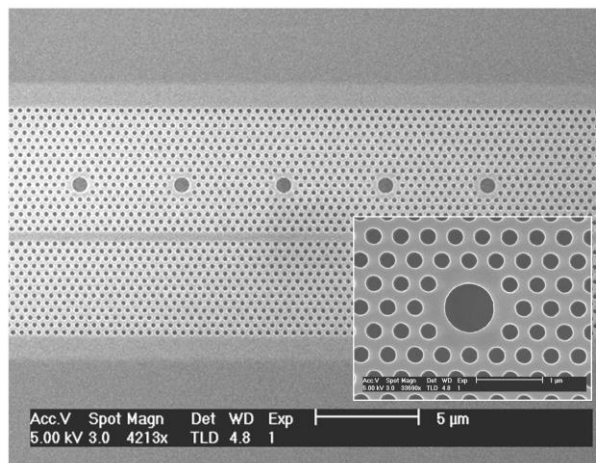
### 3.1. Photonic Crystal Arrays and Refractive Index Sensitivity Measurements

Many of the resonant waveguide sensors in the literature (for example [4–8]) utilize a single cavity as a point of reference for measuring refractive index changes. Photonic crystals, however, are small enough that multiple independent cavities can be combined in the same structure, with spacing on the order of a few microns. For example, the idea of side-coupling multiple cavities from the same bus waveguide has already been demonstrated by Mandal *et al.* [9]; here, we are taking the idea further by placing multiple cavities into the same photonic crystal (Figure 1), removing the substrate and directly attaching the fibre. Each of these cavities is excited simultaneously using a side coupling architecture in order to realise the wavelength division multiplexing approach and the ability to monitor refractive index changes as a function of both time and location. To demonstrate the multi cavity platform, we choose a “hollow cavity” design previously used for sensing [10] and optical trapping [11], due to its high sensitivity. The design parameters used here were the same as in [11], namely period  $a = 420$  nm, radius  $r \approx 125$  nm and cavity defect radius  $r_d \approx 350$  nm. Each successive cavity was made slightly larger in radius by 4 nm in order to tune the resonances to be approximately 5 nm apart in wavelength. An SEM image of a fabricated five-cavity array is shown in Figure 1.

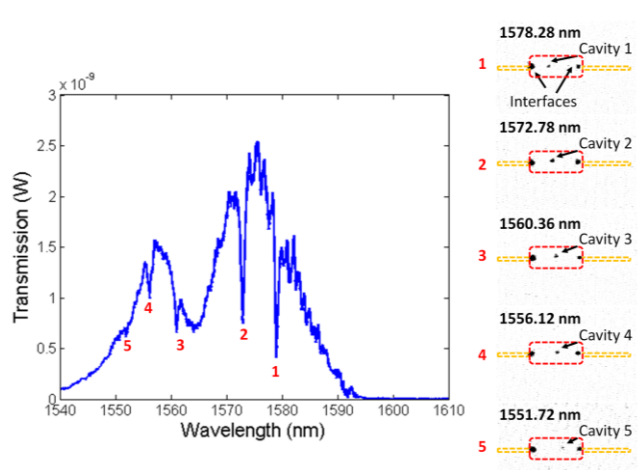
To optically characterize these waveguides, the chip was mounted in an end-fire setup, using an Amplified Spontaneous Emission (ASE) light source (33 mW, 1520–1620 nm). Light was collected from the rear of the chip with a 40x objective and sent to an optical spectrum analyser (OSA). The measured spectrum of one such device immersed in water is shown in Figure 2. Each resonant dip observed in Figure 2 was confirmed with the tuneable laser to visualize light being scattered from the respective cavity on resonance. Quality factors of approximately  $\approx 9000$  in air and  $\approx 3000$  in water were obtained. To test the refractive index sensitivity, a 40 micron high, 200 micron wide PDMS microfluidic channel was integrated onto the SOI substrate by treating the PDMS with oxygen plasma as described in [8]. Different solvents were injected, namely deionised water, methanol and ethanol, and the resonance wavelength tracked. The results for a single resonance are shown in Figure 3. From these measurements, and known values of refractive index for the solvents ( $n_{\text{methanol}} = 1.317$  [12],  $n_{\text{DI}} = 1.333$  [13–15],  $n_{\text{ethanol}} = 1.342$  [14]) the refractive index sensitivity was determined to be 200 nm/RIU from the gradient of

Figure 3b). On another sample the difference between air and deionised water was measured to be 43.5 nm (see supplementary material), which suggests a refractive index sensitivity of 130 nm/RIU. We therefore find that the refractive index sensitivity of these cavities to be between  $\approx 130\text{--}200$  nm/RIU which agrees with the  $\approx 150$  nm/RIU predicted in [11,16].

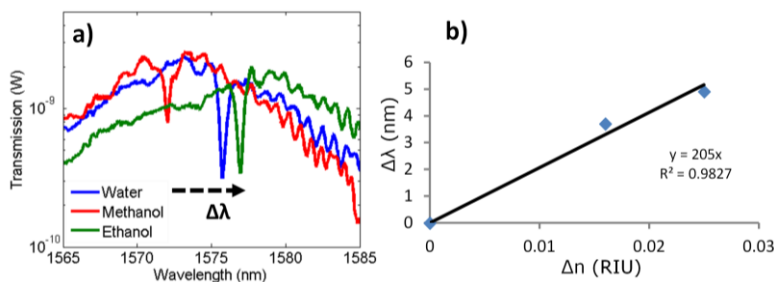
**Figure 1.** SEM images of fabricated five-cavity array.



**Figure 2.** Transmission spectrum (end-fire measurements) of five-cavity array in water highlighting each resonance and image of light scattered from each cavity location on resonance (inverted colours).



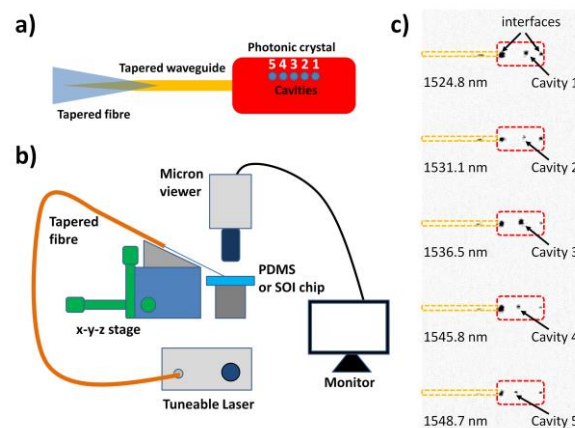
**Figure 3.** (a) Transmission spectra (log scale) for a single cavity immersed in a variety of solvents. (b) Resonance shift ( $\Delta n$ ) versus refractive index change ( $\Delta \lambda$ ) for measurements in (a).



### 3.2. Coupling to Photonic Crystal via Tapered Fibres on SOI

The results shown in Figures 2 and 3 were obtained using a free space end-fire transmission setup. Whilst end-fire is useful for fast characterization in a lab environment, it is less suitable for integrated photonics. Recently, it has been demonstrated [17] that tapered optical fibres can be used to excite inverse tapered waveguides [18] on-chip. Tapering the fibre to dimensions below that of the fibre core (6 microns for SMF28) allows the evanescent field to penetrate out of the cladding and into the air and affords evanescent coupling to another waveguide. Such tapered fibres can also be bonded directly onto the sensor without the need for angular coupling as required by grating couplers. In order to demonstrate the tapered fibre approach, we fabricated the same structure as in Figure 1 and added an inverse tapered waveguide (tapered from 50 nm to 3 microns width over a length of 100 microns) at the input end for coupling into the photonic crystal (Figure 4a). A tapered fibre was then mounted on a microblock and connected directly to the ASE, in order to actively align the fibre. To help alignment, a micronviewer IR camera and 20x objective were used to image the chip as shown in (Figure 4b). To test the different cavities, the ASE source was then exchanged for a tuneable laser, and the cavity resonances excited in sequence (Figure 4c). This highlights the ability of measuring cavity resonances that does not require a spectrometer. Instead, resonances can be tracked at different locations by imaging the light scattering from each cavity as the wavelength is tuned at the source. The uncertainty in the resonance wavelength is at worst the width of the resonance itself, which for these cavities would be 0.2 nm in air, and 0.5 nm in water. As the brightness of the cavity is at its highest at the centre of the resonance and the exciting laser can be very narrow in wavelength (for example less than 0.1 nm) the actual resolution of this technique could be much higher.

**Figure 4.** (a) Schematic of photonic crystal design and coupler. (b) Experimental setup for characterising structures on silicon-on-insulator (SOI) and polydimethylsiloxane (PDMS) using tapered fibres. (c) Light scattered from each cavity on resonance (for an SOI sample with tapers) collected by IR camera (colours inverted).



### 3.3. Photonic Waveguides Transferred to PDMS

Whilst the scheme shown in Figure 4 does not require a spectrometer to track multiple resonances, this setup necessitates using a camera and objective from above. A common constraint of photonic

waveguide structures is that they sit on a rigid and opaque substrate, for example silicon-on-insulators. For *in-situ* applications, e.g., tissue monitoring, a flexible and transparent substrate is much preferred, and we use polydimethylsiloxane (PDMS) for this purpose. PDMS is also the most popular platform for microfluidic structures and has the advantage of being flexible, biocompatible and transparent from 400 nm–2 microns. Using the method outlined in Section 2.1, photonic crystal cavity arrays were transferred onto PDMS. The resulting photonic crystal arrays on PDMS are shown in Figure 5 with images taken both in reflection and transmission.

The PDMS chip was then inserted into the setup shown in Figure 4b, and aligned to a tapered optical fibre using the microblock and camera. Each of the cavities were detected and excited independently as before using the tuneable laser and the image of the scattered light from each cavity observed by the IR camera. The resulting images are shown in Figure 6. Whilst PDMS transfer of microstructures have been shown before [19,20], this result shows that it is also possible to integrate photonic waveguides directly with PDMS. As the PDMS is highly transparent, this is particularly useful for combining with microscopy, optical traps and fluorescence applications. Using PDMS transfer reduces the amount of SOI needed, for example a chip with a long microfluidic channel would not need a large piece of silicon only a large piece of cheaper PDMS, thus higher yields can result from a piece of SOI. The mechanical flexibility of PDMS also gives another degree of freedom to open up new applications. Initial tests with two fibres, one at the input and one at the output, suggest that coupling efficiencies are comparable to end-fire coupling. Future work will involve more detailed studies of measuring and optimizing the coupling efficiency. Also of interest for future study will be the direct integration of the photonic crystal with the tapered fibre. Photonic crystals directly integrated with fibres [21,22] have recently been of interest for “lab-on-a-fibre” applications, for example for the direct probing inside a cell [21]. In that case, the fibre was used to collect light emitted from photoluminescence. The work presented here has potential for an alternative fibre probe where the fibre is instead used to excite the cavities directly. This will be the subject of future work.

**Figure 5.** Photonic crystal waveguides transferred to PDMS substrate (a) and (b) viewed in reflection and (c) viewed in transmission from light microscope.

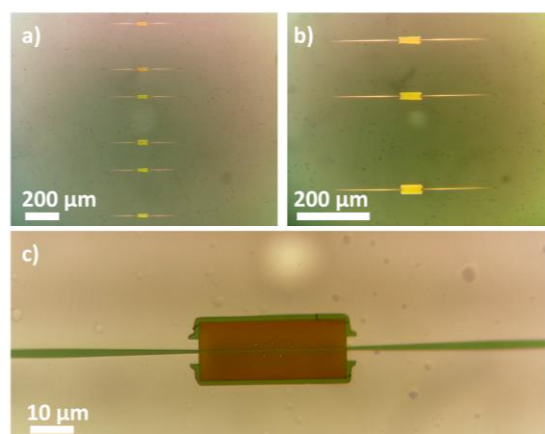
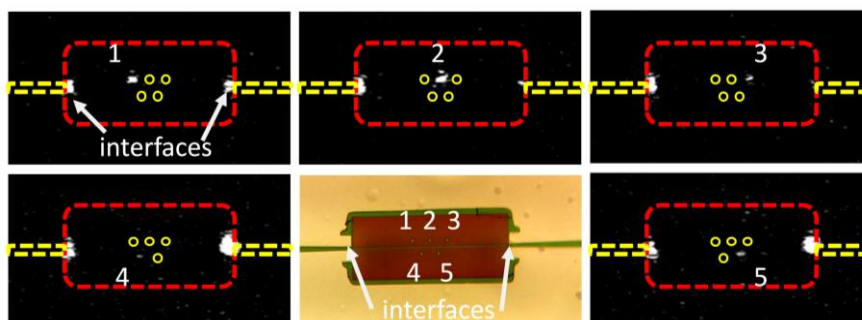


**Figure 6.** Independent excitation of multiple cavities within the same photonic crystal transferred to PDMS.



#### 4. Conclusions

In conclusion; we have demonstrated that photonic crystal waveguides can be transferred to PDMS; that multiple cavities within the same crystal can be detected using a camera for sensing as a function of location; and that tapered fibres can be used to excite these waveguides. This platform has potential for greater integration with microfluidics and microscopy than conventional wafer based photonics due to the material advantages of PDMS. Future work will focus on optimising the coupling efficiency and integrating the photonic crystals directly onto the tapered fibre.

#### Acknowledgments

We acknowledge support by the EPSRC of the UK, grant No. EP/J01771X/1 “Structured Light” for financial support.

#### Author Contributions

Mark G. Scullion contributed to the original idea, and development of the PDMS transfer; fabricated the fibres and samples, performed the measurements and drafted the paper. Matthias Fischer contributed to the fabrication of the tapered fibres, PDMS transfer, experimental setup and writing of the paper. Thomas F. Krauss contributed to the original idea, supervision of the work and the writing of the paper.

#### Conflict of Interest

The authors declare no conflict of interest.

#### References

1. De Vos, K.; Bartolozzi, I.; Schacht, E.; Bienstman, P.; Baets, R. Silicon-on-insulator resonator for sensitive and label-free biosensing. *Opt. Exp.* **2007**, *15*, 7610–7615.
2. Ksendzov, A.; Lin, Y. Integrated optics ring-resonator sensors for protein detection. *Opt. Exp.* **2005**, *30*, 3344–3346.

3. Iqbal, M.; Gleeson, M.A.; Spaugh, B.; Tybor, F.; Gunn, W.G.; Hochberg, M.; Baehr-Jones, T.; Bailey, R.C.; Gunn, L.C. Label-free biosensor arrays based on silicon ring resonators and high-speed optical scanning instrumentation. *IEEE J. Sel. Top. Quant.* **2010**, *16*, 654–661.
4. Barrios, C.A.; Gylfason, K.B.; Sanchez, B.; Griol, A.; Sohlstrom, H.; Holgado, M.; Casquel, R. Slot-waveguide biochemical sensor. *Opt. Exp.* **2007**, *32*, 3080–3082.
5. Lee, M.; Fauchet, P.M. Two-dimensional silicon photonic crystal based biosensing platform for protein detection. *Opt. Exp.* **2007**, *15*, 4530–4535.
6. Skivesen, N.; Tetu, A.; Kristensen, M.; Kjems, J.; Frandsen, L.H.; Borel, P.I. Photonic-crystal waveguide biosensor. *Opt. Exp.* **2007**, *15*, 3169–3176.
7. Toccafondo, V.; Garcia-Ruperez, J.; Banuls, M.J.; Griol, A.; Castello, J.G.; Peransi-Llopis, S.; Maquieira, A. Single-strand DNA detection using a planar photonic-crystal-waveguide-based sensor. *Opt. Exp.* **2010**, *35*, 3673–3675.
8. Scullion, M.G.; Di Falco, A.; Krauss, T.F. Slotted Photonic Crystal Cavities with Integrated Microfluidics for Biosensing Applications. *Biosens. Bioelectron.* **2011**, *27*, 101–105.
9. Mandal, S.; Goddard, J.M.; Erickson, D. A multiplexed optofluidic biomolecular sensor for low mass detection. *Lab Chip* **2009**, *9*, 2924–2932.
10. Lee, M.R.; Fauchet, P. Nanoscale microcavity sensor for single particle detection. *Opt. Exp.* **2007**, *32*, 3284–3286.
11. Descharmes, N.; Dharanipathy, U.P.; Diao, Z.; Tonin, M.; Houdre, R. Observation of Backaction and Self-Induced Trapping in a Planar Hollow Photonic Crystal Cavity. *Phys. Rev. Lett.* **2013**, *110*, 123601.
12. Kim, C.B.; Su, C.B. Measurement of the refractive index of liquids at 1.3 and 1.5 micron using a fibre optic Fresnel ratio meter. *Meas. Sci. Technol.* **2004**, *15*, 1683–1686.
13. Wei, T.; Han, Y.; Li, Y.; Tsai, H.L.; Xiao, H. Temperature-insensitive miniaturized fiber inline Fabry-Perot interferometer for highly sensitive refractive index measurement. *Opt. Exp.* **2008**, *16*, 5764–5769.
14. Lo, S.; Hu, S.; Weiss, S.M.; Fauchet, P. Photonic Crystal Microring Resonator based Sensors. In Proceedings of the CLEO: Applications and Technology, San Jose, CA, USA, 8–13 June 2014.
15. Hu, J.; Carlie, N.; Feng, N.N.; Petit, L.; Agarwal, A.; Richardson, K.; Kimerling, L. Planar waveguide-coupled, high-index-contrast, high-Q resonators in chalcogenide glass for sensing. *Opt. Exp.* **2008**, *33*, 2500–2502.
16. Dharanipathy, U.P. On the Investigation of Light-Matter Interactions in Slab Photonic Crystal Cavities. Ph.D. Thesis, Ecole Polytechnique Federale de Lausanne: Lausanne, Switzerland, 2014.
17. Groblacher, S.; Hill, J.T.; Safavi-Naenini, A.H.; Chan, J.; Painter, O. Highly efficient coupling from an optical fiber to a nanoscale silicon optomechanical cavity. *Appl. Phys. Lett.* **2013**, *103*, 181104.
18. Shoji, T.; Tsuchizawa, T.; Watanabe, T.; Yamada, K.; Morita, H. Low loss mode convertor from 0.3  $\mu\text{m}$  square Si wire waveguides to singlemode fibres. *Electron. Lett.* **2002**, *38*, 1669–1670.
19. Meitl, M.A.; Zhu, Z.T.; Kumar, V.; Lee, K.J.; Feng, X.; Huang, Y.Y.; Adesida, I.; Nuzzo, R.G.; Rogers, J.A. Transfer printing by kinetic adhesion to an elastomeric stamp. *Nat. Mater.* **2006**, *5*, 33–38.

20. Yang, H.; Zhao, D.; Chuwongin, S.; Seo, J.H.; Yang, W.; Shuai, Y.; Berrgren, J.; Hammar, M.; Ma, Z.; Zhou, W. Transfer-printed stacked nanomembrane lasers on silicon. *Nat. Photon.* **2012**, *6*, 615–620.
21. Shambat, G.; Kothapalli, S.R.; Provine, J.; Sarmiento, T.; Harris, J.; Gambhir, S.S.; Vuckovic, J. Single-Cell Photonic Nanocavity Probes. *Nano. Lett.* **2013**, *13*, 4999–5005.
22. Shambat, G.; Provine, J.; Rivoire, K.; Sarmiento, T.; Harris, J.; Vuckovic, J. Optical fiber tips functionalized with semiconductor photonic crystal cavities. *Appl. Phys. Lett.* **2011**, *99*, 191102.

© 2014 by the authors; licensee MDPI, Basel, Switzerland. This article is an open access article distributed under the terms and conditions of the Creative Commons Attribution license (<http://creativecommons.org/licenses/by/4.0/>).